Phase Identification in a Series of Liquid Crystalline TPP Polyethers and Copolyethers Having Highly Ordered Mesophase Structures. 7. Phase Structures in a Series of Copolyethers Containing Odd and Even Numbers of Methylene Units of Different Compositions

Ru-Qing Zheng,[†] Er-Qiang Chen,[†] Stephen Z. D. Cheng,*[,†] Fengchao Xie,[‡] Donghang Yan,[‡] Tianbai He,[‡] Virgil Percec,[§] Peihwei Chu,[§] and Goran Ungar[⊥]

Maurice Morton Institute and Department of Polymer Science, The University of Akron, Akron, Ohio 44325-3909; Changchun Institute of Applied Chemistry, Chinese Academy of Sciences, Changchun, Jilin, 130022, P. R. China; Department of Macromolecular Science, Case Western Reserve University, Cleveland, Ohio 44106-2699; and Department of Engineering Materials, University of Sheffield, Sheffield S1 3JD, UK

Received June 24, 1999; Revised Manuscript Received September 3, 1999

ABSTRACT: A series of liquid crystalline copolyethers have been synthesized from 1-(4-hydroxy-4′-biphenyl)-2-(4-hydroxyphenyl)propane with 1,7-dibromoheptane and 1,12-dibromododecene [coTPPs(7/12)], which represents copolyethers containing both odd and even numbers of methylene units. The molar ratio of odd to even methylene units in this series ranges from 1/9 to 9/1. The coTPPs(7/12) exhibit multiple phase transitions during cooling and heating in differential scanning calorimetry experiments. For all these thermal transitions, a small undercooling and superheating dependence is observed upon cooling and heating at different rates. Three types of phase behaviors can be classified in coTPPs(7/12) on the basis of the structural analyses by wide-angle X-ray diffraction on powder and fiber samples and by electron diffraction experiments in transmission electron microscopy. At room temperature, highly ordered smectic and smectic crystal (SC) phases are identified in coTPPs(7/12: 1/9 and 2/8), which is similar to the homopolymer TPP($m = 12$). The coTPPs(7/12: 3/7, 4/6, and 5/5) possess a hexagonal columnar (Φ_H) phase in which the molecular and columnar axes are parallel to the fiber direction and perpendicular to the hexagonal lateral packing. The coTPPs(7/12: 6/4, 7/3, and 8/2) possess a tilted hexagonal columnar (Φ_{TH}) phase with a single tilt angle which increases with the increasing composition of the seven-numbered methylene units. However, in coTPP(7/12: 9/1), a Φ_{TH} phase with multiple tilt angles is found. Upon heating, phase structures in most coTPPs(7/12) involving the columnar phases enter directly into the nematic (N) phase, while the coTPP(7/12: 1/9) exhibits a highly ordered smectic F (S_F) phase before it reaches the N phase. One exception is found in coTPP(7/12: 2/8), wherein the transformation from the S_F to Φ_H occurs prior to the N phase. Combining the copolymer phase behaviors observed with the corresponding homopolymers TPP($n = 7$) and TPP($m = 12$), a phase diagram describing transition temperatures with respect to the composition can be constructed.

Introduction

In the previous publications, we have reported the phase identification of a series of main-chain liquid crystalline polyethers synthesized from 1-(4-hydroxy-4′-biphenyl)-2-(4-hydroxyphenyl)propane and α,ω-dibromoalkanes [TPP(*n*)], where highly ordered smectic F (S_F), smectic crystal G (SC_G), and H (SC_H) phases have been assigned.[1−3] The phase structures and transition behaviors are different for TPPs with odd and even numbers of methylene units. For example, the transitions of TPP($n = 7$) follow the sequence[2]

$$\text{glassy state} \leftrightarrow SC_G \leftrightarrow S_F \leftrightarrow N \leftrightarrow I$$

compared to the TPP($m = 12$) sequence[3]

$$\text{glassy state} \leftrightarrow K_2 \leftrightarrow K_1 \leftrightarrow SC_H \leftrightarrow SC_G \leftrightarrow S_F \leftrightarrow I$$

Phase behavior of TPP($m = 12$) differs from TPP($n = 7$) in that when TPP($m = 12$) is cooled from the isotropic melt (I), a S_F phase is developed directly without the formation of a N phase. Another difference is related to the chain orientation: S_F and SC_G phases in TPP($n = 7$) possess the molecular axis tilted approximately 14° from the fiber direction,[2] whereas in all phases of TPP($m = 12$), the molecular axis is parallel to the fiber direction as evidenced in the wide-angle X-ray diffraction (WAXD) fiber patterns.[3] Furthermore, TPP($m = 12$) possesses two crystalline phases, K_1 and K_2, which do not exist in TPP($n = 7$). The transition thermodynamic properties (temperatures and heats of transitions) are also different in these TPPs.[2−6] Molecular dynamics in different phases,[7] surface-induced phase structures,[8,9] and structural and morphological development in TPPs[8,9] have also been investigated.

The first examples of columnar liquid crystals were prepared and identified in small molecular disklike compounds in 1977,[10] where the disks were found to be stacked one on top of the other, aperiodically forming liquidlike columns. These different columns constituted a two-dimensional lattice. Most of the studies on columnar phases have been focused on molecules with disk-shaped mesogens.[11−16] Polymers possessing discotic mesogens both in main chains and as side groups also become a topic of considerable interest.[17,18] The colum-

[†] The University of Akron.
[‡] Chinese Academy of Sciences.
[§] Case Western Reserve University.
[⊥] University of Sheffield
* To whom correspondence should be addressed.

10.1021/ma9910235 CCC: $18.00
Published on Web 10/01/1999

nar liquid crystals, also referred to as discotic liquid crystals, are characterized by the existence of long-range order in two dimensions and an absence of order in the third dimension. Compared to homopolymers, copolymers with various methylene unit lengths can generate aperiodicity along the chain direction and may exhibit columnar phases in the case of the rodlike mesogens.

The various combinations of comonomers with different numbers of methylene units can generally classify TPP copolyethers into three types: copolyethers containing both odd- and even-numbered methylene units and the copolyethers containing either only odd- or only even-numbered methylene units. The different spacer lengths may also significantly change the phase structures and transition behaviors. The current study has been particularly encouraged by our recent work on a series of coTPP(n/m)s containing a fixed even ($m = 12$) and varying odd numbers ($n = 5$, 7, 9, and 11) of methylene units with their compositions fixed at an equal molar ratio (5/5).[19] In that study, the SC phases are retained when the dissimilarity of the comonomer lengths is small, as in coTPP(11/12: 5/5). However, a hexagonal columnar (Φ_H) phase is identified for the increasing dissimilarity, and thus, the defects due to the mismatch of the mesogenic groups destroy the third dimensional long-range order along the molecular direction, as in coTPPs(5/12: 5/5 and 7/12: 5/5).

In this publication, nine coTPPs studied have the following chemical structures with both fixed odd ($n = 7$) and even ($m = 12$) numbers of methylene units:

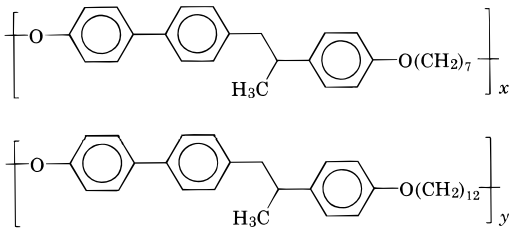

By changing the molar ratio (x/y) from 1/9 to 9/1, the composition effect on the phase structure and transition behavior is investigated. It is expected that we may further understanding of new phase identifications and classifications by studying this series of coTPPs(7/12).

Experimental Section

Materials. The series of coTPPs(7/12) were synthesized by random copolymerization from 1-(4-hydroxy-4′-biphenyl)-2-(4-hydroxyphenyl)propane (TPP) with 1,7-dibromohexene and 1,12-dibromododecene. The detailed synthetic procedure of homoTPPs has been reported in an earlier publication.[20] The relative number-average molecular weights (M_n) of coTPPs-(7/12) ranged from 20 000 to 30 000 g/mol as determined via gel permeation chromatography (GPC) based on polystyrene standards.

Instruments and Experiments. The thermal transition behaviors were detected via a Perkin-Elmer DSC-7 instrument. The temperature and heat flow were calibrated using standard materials at different cooling and heating rates between 2.5 and 40 °C/min. Samples with a typical mass of 2−3 mg were encapsulated in sealed aluminum pans. When fast cooling and heating rates were applied, the sample mass was reduced to less than 1 mg to avoid any sample thermal gradients. A controlled cooling experiment was always run first, followed by heating performed at a rate that was equal to or faster than the prior cooling. The equilibrium transition temperatures were determined by extrapolating the onset temperatures to a rate of 0 °C/min.

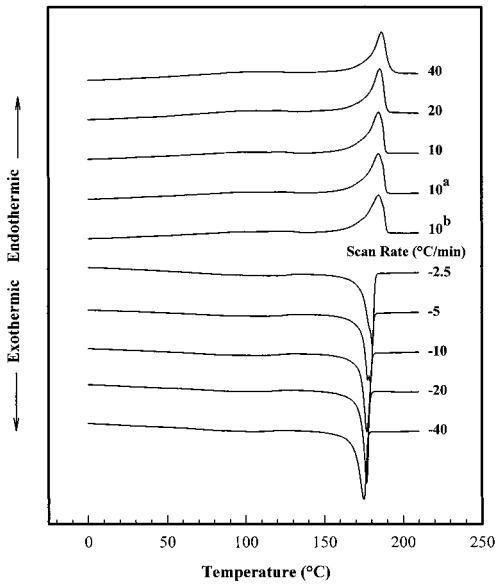

Figure 1. Set of DSC curves of coTPP(7/12: 1/9) at different cooling and heating rates. 10^a: the heating rate after cooling at 5 °C/min; 10^b: the heating rate after cooling at 2.5 °C/min.

WAXD powder experiments were performed with a Rigaku 12 kW rotating anode generator (Cu Kα radiation) equipped with a Geigerflex D/max-RB diffractometer. A hot stage in conjunction with the diffractometer was used to study the structural evolution as a function of temperature. The temperature was controlled to less than ±1 °C. Films of approximately 0.1 mm in thickness were mounted on aluminum sheets, and the diffraction patterns were collected in the reflection mode. Samples were scanned in a 2θ range between 2° and 30°. Background scattering was recorded and subtracted from WAXD patterns.

Fibers were prepared by drawing the samples from the N phase for the purpose of phase structure determination. A fiber diameter of 30 μm was typical. WAXD fiber patterns were obtained from a Rigaku automated X-ray imaging system with 3000 × 3000 pixel resolution. A 30 min exposure was required for the WAXD fiber patterns. The air scattering was collected separately and subtracted.

Phase morphology and liquid crystalline defects were examined with a polarized light microscope (PLM) (Olympus BH-2) coupled with a Mettler hot stage (FP-90) and a JEOL, JEM-120 transmission electron microscope (TEM). Both isothermal and nonisothermal experiments were performed for PLM observation of thin films obtained by melt-pressing small amounts of samples between two glass slides. To study the liquid crystalline morphological changes under an external force field, several mechanically sheared samples were used. The TEM was operated at an accelerating voltage of 120 kV. The TEM samples were solution cast on amorphous carbon-coated surfaces at a concentration of 0.1% (w/w) in tetrahydrofuran. After the solvent evaporation, the thin films were heated and held in the N phase for 15 h, slowly cooled, shadowed with Pt, and finally coated with carbon. Calibration of the electron diffraction (ED) spacings in TEM was carried out using Au and TlCl in a d spacing range less than 0.384 nm, the largest spacing for TlCl. Spacing values greater than 0.384 nm were calibrated by doubling the d spacings of those reflections based on their first-order reflections.

Results and Discussion

Transition Properties in coTPPs(7/12). Figure 1 includes both sets of heating and cooling DSC curves of coTPP(7/12: 1/9) as an example. Two major exothermic and endothermic peaks are observed during cooling and heating, respectively. However, the transition at approximately 180 °C consists of actually two peaks, which

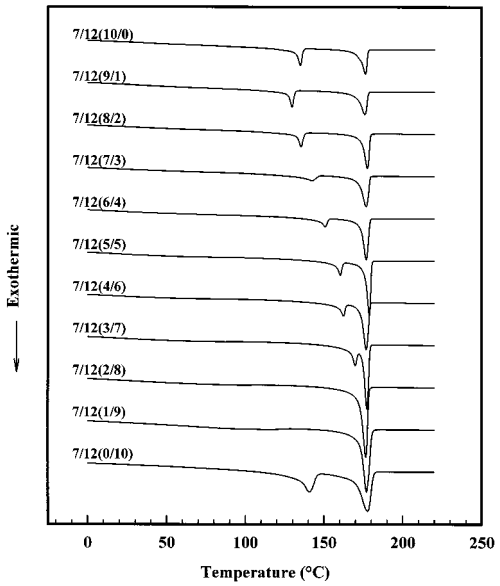

Figure 2. Set of DSC cooling curves for all coTPPs(7/12) and homoTPPs($n = 7$ and $m = 12$) at 10 °C/min.

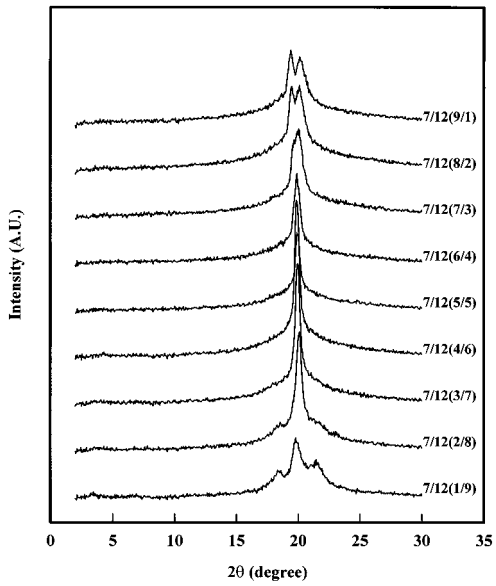

Figure 3. WAXD powder patterns of coTPPs(7/12) taken at room temperature after the samples were cooled from the isotropic melt at 2.5 °C/min.

is evident on slow cooling. A broad transition starts at approximately 130 °C on cooling and is also observed on heating. All the transitions exhibit a small cooling and heating rate dependence. In general, the undercooling of the onset transition temperatures observed between 2.5 and 40 °C/min is within 1−2 °C. Figure 2 presents the DSC cooling thermodiagrams of all coTPPs(7/12) at a rate of 10 °C/min. The thermodiagrams of both homoTPPs($n = 7$ and $m = 12$) are also included for comparisons. Compared with the homoTPP($m = 12$), the low-temperature transitions in coTPPs(7/12: 1/9 and 2/8) (at approximately 130 and 110 °C, respectively) show much broader and smaller exothermic peaks, corresponding to a decrease in the transition enthalpy change. Such low-temperature transitions become experimentally difficult to detect by DSC when the composition of TPP($n = 7$) exceeds 30%. (It is not clear in Figure 2 due to the heat-flow scale.) To construct the phase diagram from this series of coTPPs(7/12), identification of each phase structure is required.

Ordered Structures at Room Temperature. Figure 3 shows a set of WAXD powder patterns obtained at room temperature after the samples were cooled from the isotropic melt at 2.5 °C/min. The copolymers can be categorized into three groups on the basis of their diffraction patterns. CoTPPs(7/12: 1/9 and 2/8) belong to the first group, wherein three reflections in the wide-angle region and one reflection in the low-angle region are evident. The second group contains coTPPs(7/12: 3/7, 4/6, and 5/5), each of which exhibits only one single, sharp reflection at a 2θ of approximately 20°. The third group of coTPPs(7/12: 6/4, 7/3, 8/2, and 9/1) has a single wide-angle reflection which splits into two. The two separated reflections of coTPP(7/12: 9/1), in particular, can be clearly observed with a relatively broad full width at half-maximum. It is important to note that these powder patterns are not sufficient to perform structure determinations due to the lack of information of lattice dimensionality.

Figure 4a−d illustrates the room temperature WAXD fiber patterns of coTPPs(7/12: 1/9, 4/6, 8/2, and 9/1), which are typical of the three groups of coTPP(7/12) series. However, the coTPP(7/12: 9/1) is a special case of the third group (see below). Note that, in most of

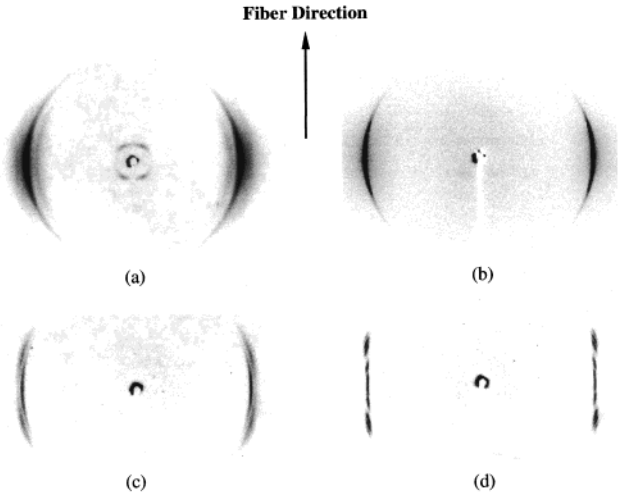

Figure 4. Room-temperature WAXD fiber patterns of (a) coTPP(7/12: 1/9), (b) coTPP(7/12: 4/6), (c) coTPP(7/12: 8/2), and (d) coTPP(7/12: 9/1).

highly ordered smectic and smectic crystal phases, the number of WAXD reflections is limited. The fit of unit cell based on these reflections is thus usually in good agreement. The fiber pattern of coTPP(7/12: 1/9) (Figure 4a) demonstrates one intense reflection at $2\theta = 19.8°$ (d spacing of 0.45 nm) on the equator and two reflections at $2\theta = 17.9°$ and 21.7° (d spacings of 0.49 and 0.41 nm, respectively) in the quadrants. The first- and second-order layer reflections can be observed at $2\theta = 3.6°$ and 7.1° (d spacings of 2.48 and 1.24 nm), which are tilted 35° from the meridian (i.e., the fiber direction). The structure of coTPP(7/12: 1/9) at room temperature can be determined following the same procedure used in homoTPP($m = 12$).[3] Hexagonal lateral packing is found perpendicular to the fiber direction. Assuming an orthorhombic lattice, the equatorial reflection is assigned as the superimposed (200) and (110) reflections. The molecular axis is therefore parallel to the fiber direction. The two reflections in the wide-angle region in the first layer of the quadrants originate from the ($\bar{2}01$) and (201) planes. Since the layer reflections lie at

Table 1. Highly Ordered Smectic and Smectic Crystal Phases in CoTPPs(7/12: 1/9 and 2/8)

coTPP(7/12) (x/y)	(hkl)	2θ (deg)	d spacing (nm)	unit cell parameters
(1/9)	(001)	3.6	2.48	$a = 1.10$ nm
	(002)	7.1	1.24	$b = 0.52$ nm
	(200)	19.8	0.45	$c = 3.03$ nm
	($\bar{2}$01)	21.7	0.41	$\beta = 125°$
	(201)	17.9	0.49	(monoclinic)
(2/8)	(001)	3.7	2.42	$a = 1.13$ nm
	(002)	7.2	1.22	$b = 0.51$ nm
	(200)	19.9	0.45	$c = 3.07$ nm
	($\bar{2}$01)	22.2	0.40	$\beta = 128°$
	(201)	17.7	0.50	(monoclinic)

an angle of 35° from the meridian, the layer surface normal possesses a 35° angle with respect to the molecular orientation (also the fiber direction). Within the layers, the chain molecules are thus tilted toward one side of the hexagon, which results in $a > b$. WAXD data analysis shows that all of the observed reflections fit into a monoclinic unit cell with $a = 1.10$ nm, $b = 0.52$ nm, $c = 3.03$ nm, and $\beta = 125°$. This is a SC_G phase according to the classifications in small molecular liquid crystals.[21,22] The assignment can also be supported by tilting experiments in TEM, wherein the hexagonal ED patterns indicate a hexagonal lateral packing.

The a and b dimensions of coTPP(7/12: 1/9) are similar to the homopolymers [$a = 1.05$ nm and $b = 0.54$ nm for TPP($n = 7$),[2] and $a = 1.08$ and $b = 0.53$ nm for TPP($m = 12$)[3]]. The layer spacings of homoTPPs($n = 7$ and $m = 12$) are 1.89 and 3.27 nm, respectively. The c dimension of the coTPP(7/12: 1/9) is 3.03 nm and is intermediate between those of the homopolymers, being much closer to that of TPP($m = 12$). This is reasonable since only 10% of the TPP($n = 7$) comonomer composition is involved. Moreover, the layer normal in the copolymer is tilted at a slightly larger angle with respect to the fiber direction than those of the homoTPPs [$\beta = 125°$ for the copolymer vs $\beta = 120°$ for TPP($n = 7$) and 121° for TPP($m = 12$)]. CoTPP(7/12: 2/8) at room temperature is assigned as a S_F phase possessing a monoclinic unit cell on the basis of the structural similarity with the corresponding homoTPPs. Table 1 lists the unit cell dimensions of both coTPPs(7/12: 1/9 and 2/8) in the smectic and smectic crystal phases. Two-chain monoclinic unit cells give rise to the calculated densities that fit well with the density measurements. Note that the layer normal is further tilted with the involvement of increasing composition of TPP($n = 7$).

In the coTPP(7/12: 4/6) fiber pattern (Figure 4b), a sharp equatorial reflection appears at $2\theta = 19.9°$ (d spacing of 0.45 nm). This single reflection is attributed to a hexagonal lattice in a two-dimensional array perpendicular to the molecular axis. Therefore, this reflection represents again the superimposed (110) and (200) reflections. The hexagonal lattice can be proven by the observation of another weak but sharp equatorial reflection at a 2θ of approximately 35° (d spacing of 0.26 nm, not shown in Figure 4b). The ratio of these two d spacings yields a value of $\sqrt{3}$, which is characteristic of hexagonal packing. However, the layer spacing cannot be determined since only weak and diffuse streaks in the quadrants are observed in the low-angle region. The sharp, narrow lateral reflection and the diffuse layer streaks indicate long-range positional order along the lateral array and a lack of such an order along the third direction;[23−25] therefore, a hexagonal columnar phase (Φ_H) is identified. The calculation leads to the dimensions of $a = 0.89$ nm, $b = 0.51$ nm, and $\beta' = 90°$, where β' represents the angle between the a axis and column direction. The suppression of the highly ordered smectic phase can be attributed to the dissimilarity in methylene unit lengths of the comonomers.

Table 2. Hexagonal Columnar Phases in CoTPPs(7/12: 3/7, 4/6, and 5/5)

coTPP(7/12) (x/y)	(hk0)	2θ (deg)	d spacing (nm)	unit cell parameters
(3/7)	(200)	19.9	0.45	$a = 0.89$ nm, $b = 0.51$
	(110)			nm, $\beta' = 90°$
(4/6)	(200)	19.9	0.45	$a = 0.89$ nm, $b = 0.51$
	(110)			nm, $\beta' = 90°$
(5/5)	(200)	19.9	0.45	$a = 0.89$ nm, $b = 0.52$
	(110)			nm, $\beta' = 90°$

Similar identification can be carried out in coTPPs-(7/12: 3/7 and 5/5), where the ordered structures at room temperature are also categorized as a Φ_H phase. Table 2 summarizes the room temperature structural dimensions in coTPPs(7/12: 3/7, 4/6, and 5/5). It is evident that their lateral hexagonal lattice dimensions are virtually identical. Their columnar axes lie on the hexagonal packing normal and are all parallel to the molecular direction. The Φ_H phase in coTPP(7/12: 5/5) has been previously determined.[19]

Unlike the copolymers discussed above, the fiber pattern of coTPP(7/12: 8/2) (Figure 4c) presents no reflection on the equator but rather two reflections in the quadrants. The appearance of two reflections is caused by the split of the (110) and (200) reflections due to a tilted unit cell with respect to the fiber direction as in several homoTPPs.[1−3] In the coTPP(7/12: 8/2) fiber pattern, the (200) reflection at $2\theta = 20.1°$ (d spacing of 0.44 nm) is tilted 17° from the equator, whereas the (110) reflection at $2\theta = 19.4°$ (d spacing of 0.46 nm) is tilted approximately 8° from the equator. No low-angle layer reflections can be experimentally observed, indicating that the layer structure in this sample has been significantly disturbed with the further incorporation of the TPP($n = 7$) comonomer. Note that the degree of tilt from the equator of the (110) and (200) reflections, the ratio of these two corresponding d spacings, and the tilt of molecular axis possess a fixed geometric relationship. Our calculation shows that in the coTPP(7/12: 8/2) the hexagonal lateral packing is maintained along the cross section perpendicular to the fiber direction, and the molecular chain axis is tilted 17° from the normal of hexagonal lattice. Since the molecular axis represents the preferred direction of chain orientation, the tilted direction with respect to the hexagonal normal therefore leads to the identification of a tilted, hexagonal columnar (Φ_{TH}) phase. The dimensions perpendicular to the fiber direction of this Φ_{TH} lateral array are $a = 0.92$ nm and $b = 0.53$ nm. The β' angle between the a axis and column direction is 107°.

CoTPPs(7/12: 6/4 and 7/3) exhibit similar fiber patterns to that of coTPP (7/12: 8/2), possessing the Φ_{TH} phase. Their detailed dimensional parameters are listed in Table 3. In this table, the d spacing ratios of the (110) and (200) reflections based on the calculation of the hexagonal lattice are also listed, which are in good agreement with experimental data. Both the a and b dimensions and the tilt angle β' slightly increase with increasing TPP($n = 7$) comonomer composition.

Table 3. Tilted Hexagonal Columnar Phases in CoTPPs(7/12: 6/4, 7/3, and 8/2)

coTPP(7/12) (x/y)	($hk0$)	($hk0$) wrt equator (deg)	d spacing (nm)	unit cell parameters	$d_{(200)}/d_{(110)}$ (calculated)	$d_{(200)}/d_{(110)}$ (measured)
(6/4)	(200)	9	0.449	$a = 0.91$ nm, $b = 0.53$ nm, $\beta' = 99°$	0.991	0.991
	(110)	4	0.453			
(7/3)	(200)	13	0.445	$a = 0.91$ nm, $b = 0.53$ nm, $\beta' = 103°$	0.980	0.978
	(110)	6	0.455			
(8/2)	(200)	17	0.442	$a = 0.92$ nm, $b = 0.53$ nm, $\beta' = 107°$	0.967	0.965
	(110)	8	0.458			

Table 4. Tilted Hexagonal Columnar Phases in CoTPP(7/12: 9/1)

	($hk0$)	($hk0$) wrt equator (deg)	d spacing (nm)	unit cell parameters	$d_{(200)}/d_{(110)}$ (calculated)	$d_{(200)}/d_{(110)}$ (measured)
(1)	(200)	22.5	0.432	$a = 0.93$ nm, $b = 0.54$ nm, $\beta' = 112.5°$	0.943	0.942
	(110)	11	0.458			
(2)	(200)	19.5	0.439	$a = 0.93$ nm, $b = 0.54$ nm, $\beta' = 109.5°$	0.957	0.957
	(110)	10	0.458			
(3)	(200)	17	0.444	$a = 0.93$ nm, $b = 0.54$ nm, $\beta' = 107°$	0.969	0.967
	(110)	8	0.460			
(4)	(200)	4	0.464	$a = 0.93$ nm, $b = 0.54$ nm, $\beta' = 94°$	0.998	0.998
	(110)	2	0.465			

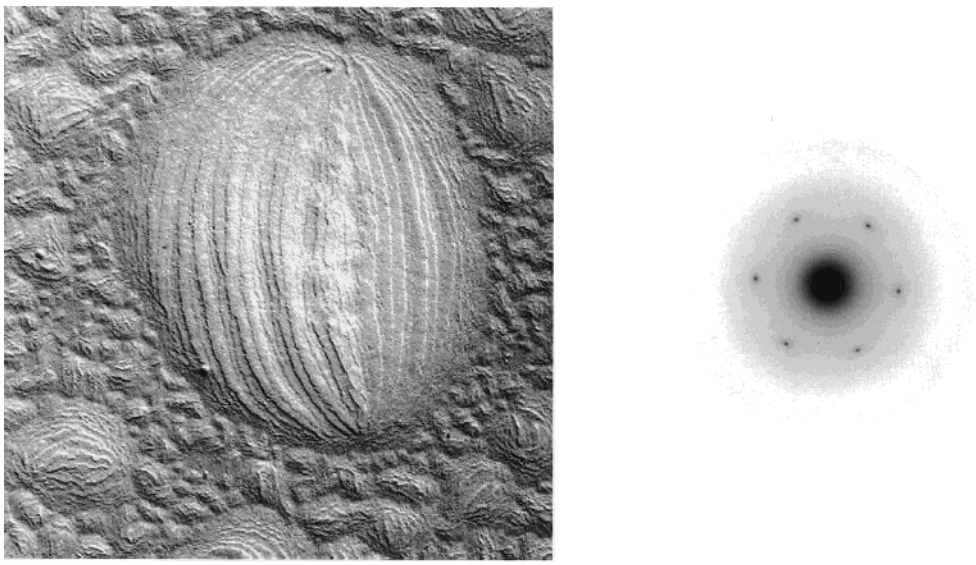

Figure 5. TEM morphological observation and tilted ED result from coTPP(7/12: 9/1).

The Φ_{TH} can still be assigned in coTPP(7/12: 9/1), although its fiber pattern (Figure 4d) is different from the one shown in Figure 4c. Multiple reflections in the quadrants are observed on a pair of "lines" that are nearly parallel to the meridian. They correspond to the two reflection peaks in WAXD powder pattern, which possess relatively broad peak widths due to the overlap. These reflections can be separated into four sets, each of which includes the (200) and (110) reflections. The structural analysis indicates a Φ_{TH} phase with varying tilt angles. As shown in Table 4, the calculated ratio of each set of d spacings assuming hexagonal packing is consistent with the WAXD experimental measurements. Surprisingly, the hexagonal lateral array dimensions for these four sets of reflections are identical: $a = 0.93$ nm and $b = 0.54$ nm. Four different tilt angles are determined: $\beta' = 94°$, 107°, 110°, and 113°. CoTPP(7/12: 9/1) can be thus visualized as clusters of columns, the cross section of which is a hexagonal lattice, but columns tilted from the hexagonal normal at different angles. Compared with the Φ_H phase in coTPPs(7/12: 3/7, 4/6, and 5/5), the layer structure of the Φ_{TH} phase in coTPPs-(7/12: 6/4, 7/3, 8/2, and 9/1) is further destroyed and experimentally unobservable. This may be explained by the fact that the homoTPP($n = 7$) shows weaker layer reflection than the homoTPP($m = 12$).

ED experiments in TEM also support the assignment of a hexagonal lattice in the Φ_{TH} phase. Figure 5 shows the selective area ED pattern of coTPP(7/12: 9/1). The hexagonal ED pattern can be obtained by the tilting experiment. The droplet is the common morphology in the sample. It is speculated that microphase separation occurs in coTPP(7/12: 9/1), generating different domains of varying compositions. A thorough comonomer sequence analysis of this copolymer is necessary prior to drawing any conclusion.

Structural Evolution during Heating. Figure 6a−c shows three sets of WAXD powder patterns during heating at 2.5 °C/min for coTPPs(7/12: 1/9, 4/6, and 8/2). The powder pattern of coTPP(7/12: 1/9) (Figure 6a) exhibits three major reflections in the wide angle region at room temperature with 2θ values of 17.9°, 19.8°, and 21.7°, corresponding to the $(\bar{2}01)$, (200)/(110), and (201) reflections as discussed previously. In the low-angle region, a reflection appears at $2\theta = 3.6°$ (d spacing of 2.48 nm), which is attributed to the layer reflection observed in the fiber pattern (Figure 4a). This phase has been identified as a SC_G phase. The (200)/(110)

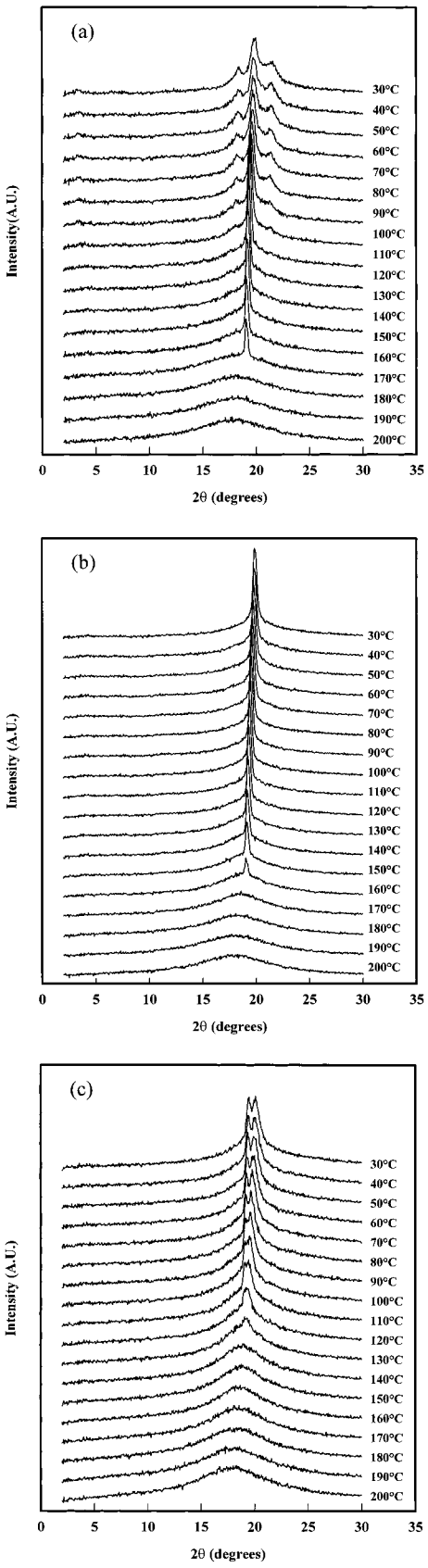

Figure 6. WAXD powder patterns for (a)coTPP(7/12: 1/9), (b)coTPP(7/12: 4/6), and (c) coTPP(7/12: 8/2) at various temperatures.

reflections narrow with increasing temperature, in contrast to the ($\bar{2}$01) and (201) reflection intensities which gradually decrease. At approximately 130 °C, the ($\bar{2}$01) and (201) reflections almost disappear with the sharp, intense (200)/(110) reflections remaining only. This indicates that within the smectic layers the crystal gradually decreases its third dimensional order along the *c* axis but remains its order in the lateral *ab* plane. The layer reflection at $2\theta = 3.6°$ survives upon heating above 130 °C, as indicated in the fiber patterns, but is less evident in the WAXD powder patterns. Consequently, the sample lacks three-dimensional long range order and is transformed into a smectic phase,[21,22] revealing a $SC_G \rightarrow S_F$ phase transition.

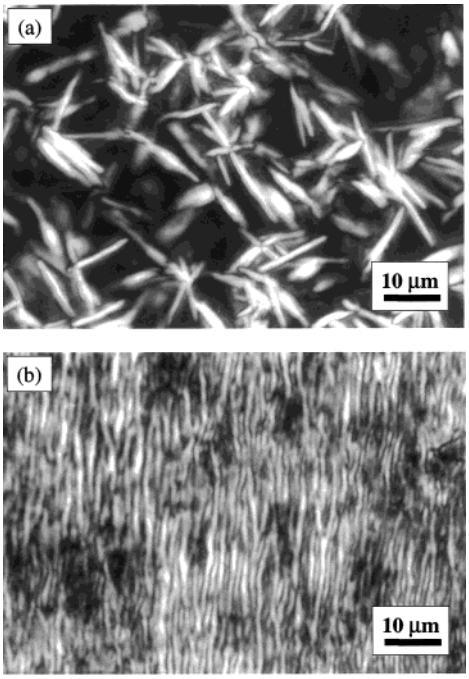

Figure 7. PLM morphological observations of coTPP(7/12: 1/9): (a) a S_F phase without mechanical shearing; (b) banded textures after mechanical shearing. The shear direction is horizontal.

The (200)/(110) reflections then continuously decrease in intensity upon further heating and are no longer evident at approximately 180 °C, coinciding with a disappearance of the layer reflection. This represents a $S_F \rightarrow N$ phase transition. A 10% composition of TPP($n = 7$) is responsible for generating the N phase, since pure TPP($m = 12$) does not exhibit this phase. Further heating brings a shift of the amorphous scattering halo to a lower 2θ value, indicating a transition of the N phase to the I melt. This has been observed in many liquid crystalline polymers,[26−29] including the homo-TPPs[1−3] and coTPPs.[19] However, since the last two transitions in coTPP(7/12: 1/9) are superimposed within a narrow temperature region (see DSC results from Figure 1), a precise separation of these two phase transformations is difficult under the temperature resolution of the WAXD experiments.

The N phase in coTPP(7/12: 1/9) can, however, be identified using PLM. Parts a and b of Figure 7 illustrate the PLM observations of the phase morphologies in coTPP(7/12: 1/9). Upon cooling from the melt, the highly ordered S_F morphology is directly developed without the appearance of two and four brushes in the schlieren texture (Figure 7a). On the other hand, the mechanically sheared sample at 181 °C produces banded textures perpendicular to the shear direction following a slight relaxation of the molecules (Figure 7b). Since the banded textures under an external force field can only be obtained when a sample is in a low ordered

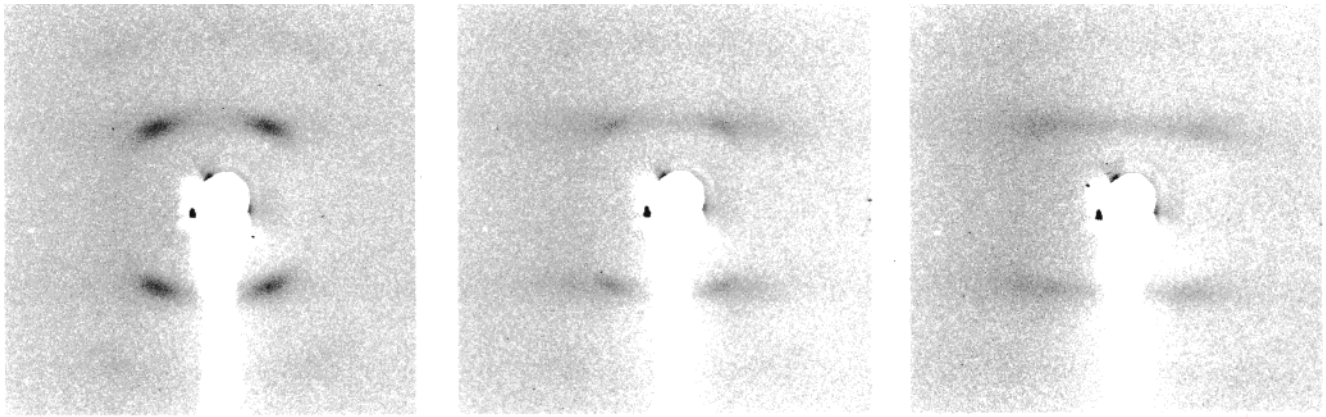

Figure 8. Layer structure change of coTPP(7/12: 2/8) as shown in WAXD fiber patterns during heating: (a) 100, (b) 110, and (c) 120 °C.

liquid crystalline phase, this observation provides indirect evidence for the existence of a N phase in this copolymer. This assignment is also supported by the transition enthalpy change, which corresponds to the additive enthalpy values of the $S_F \rightarrow N$ and $N \rightarrow I$ transitions. All of the transition temperatures in PLM experiments are consistent with the DSC measurements (see Figures 1 and 2). Therefore, the transition sequence of coTPP(7/12: 1/9) is

$$\text{glassy state} \leftrightarrow SC_G \leftrightarrow S_F \leftrightarrow N \leftrightarrow I$$

The diffraction behavior of coTPP(7/12: 2/8) during heating is similar to that of the coTPP(7/12: 1/9). The ($\bar{2}$01) and (201) reflections in the wide-angle region gradually decrease in intensity and finally disappear at approximately 110 °C. Only the superimposed (200)/(110) reflections at $2\theta = 19.9°$ remain sharp but also vanish at temperatures exceeding 180 °C. However, the coTPP(7/12: 2/8) is the only sample in this series that exhibits the smectic to columnar phase transition. The layer structure evolution shown in the WAXD fiber patterns upon heating (Figure 8) describes this type of transition. The spotlike layer reflection in the low-angle region at 100 °C changes to the diffuse streaks at 120 °C, which is consistent with our earlier work.[19] The transition sequence of coTPP(7/12: 2/8) is

$$\text{glassy state} \leftrightarrow S_F \leftrightarrow \Phi_H \leftrightarrow N \leftrightarrow I$$

WAXD powder patterns of coTPP(7/12: 4/6) recorded during heating (Figure 6b) demonstrate only one sharp Bragg reflection at 2θ of approximately 19.9°, which is a Φ_H phase in character. The low-angle reflection that indicated by the weak and diffuse streaks in the fiber pattern (Figure 4b) is difficult to observe in powder patterns. Upon heating, the intensity of the (200)/(110) reflections increases initially before decreasing at approximately 110 °C. The reflections disappear when the temperature reaches 170 °C, corresponding to a $\Phi_H \rightarrow N$ phase transition. The sudden shift of the scattering halo can be identified at approximately 180 °C at the $N \rightarrow I$ phase transition. The transition temperatures in WAXD experiments agree with the DSC results (Figure 2). Similar observations can be made in coTPPs(7/12: 3/7 and 5/5). The phase transition sequence for these three coTPPs is

$$\text{glassy state} \leftrightarrow \Phi_H \leftrightarrow N \leftrightarrow I$$

The low-angle diffuse streaks in the Φ_H phase for the coTPPs (7/12: 3/7, 4/6, and 5/5) may be attributed to the residuals of the layer structures. Their appearance implies the disturbance caused by both the mismatch of the methylene units lengths and the composition change.

Two reflections in the wide-angle region are observed in coTPP(7/12: 8/2) (Figure 6c). These represent the split (200) and (110) reflections, and a Φ_{TH} phase is assigned for the sample at room temperature. The two reflections gradually decrease in intensity and tend to merge together when the temperature increases. No Bragg reflections are observed over the 2θ region studied for temperatures above 140 °C. As is the case for all of the copolymers in this series, the $N \rightarrow I$ phase transition occurs at approximately 180 °C, accompanied by the sudden shift of the scattering halo. The coTPPs-(7/12: 6/4, 7/3, and 9/1) exhibit identical transition behavior, although the Φ_{TH} phase of coTPP(7/12: 9/1) possesses multiple tilt angles between the molecular axes and the *a* axis. The phase transition sequence for these four coTPPs can be summarized as follows:

$$\text{glassy state} \leftrightarrow \Phi_{TH} \leftrightarrow N \leftrightarrow I$$

The phase diagram (Figure 9) of coTPPs(7/12) can be constructed by plotting equilibrium temperatures as a function of the composition. The T_g's of all coTPPs(7/12) fall into the region of 40−50 °C, which are intermediate between those of TPP($n = 7$) and TPP($m = 12$).

Conclusion

A series of coTPPs(7/12) were examined to study the effects of the mismatch of the spacer lengths and the composition change on the phase structures and transition behaviors simultaneously. The structures and transitions are different from the corresponding homoTPPs($n = 7$ and $m = 12$). Three major effects were observed: (1) When a small amount of TPP($n = 7$) is incorporated, such as in the case of coTPPs(7/12: 1/9 and 2/8), the chain packing is not substantially disturbed. This results in the formation of highly ordered smectic phases such as the SC_G and S_F phases. (2) For compositions of TPP($n = 7$) between 30% and 50%, the smectic phases are suppressed, and a Φ_H phase appears as a stable phase. In this Φ_H phase, the molecular axis

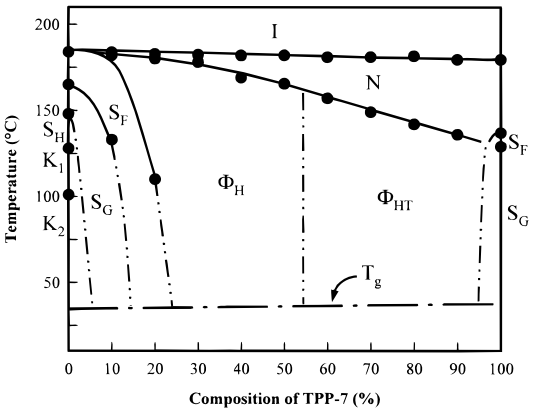

Figure 9. Phase diagram of coTPPs(7/12).

is parallel to the fiber direction, which is identical to the normal of *ab* plane. (3) For compositions of TPP(n = 7) comonomer exceeding 50%, the molecular axis is tilted from the normal of the hexagonal lateral packing plane, leading to a Φ_{TH} phase. Since the coTPP(7/12) series contains only elongated anisotropic mesogenic groups, the identification of columnar phases in these polymers provides evidence that a disk shape of mesogen is not necessarily required to generate a columnar phase. To the best of our knowledge, this is the first time that a Φ_{TH} phase in a main-chain liquid crystalline polymer has been observed.

It is evident through this study that not only the copolymerization leads to a significant disturbance of the layer structural ordering but also the odd- and even-numbered methylene units play disproportionate roles to the phase structures and transition behaviors. The composition of TPP(n = 7) is more closely related to the tilted molecular axes in copolymers; TPP(m = 12) comonomer can more effectively disturb the layer ordering since only 10% of the TPP(m = 12) comonomer results in the formation of a Φ phase, whereas it takes 30% of the TPP(n = 7) to achieve such a phase.

Acknowledgment. This work was supported by the National Science Foundation (DMR-96-17030) and the Science and Technology Center for Advanced Liquid Crystal Optical Materials (ALCOM) at Kent State University, Case Western Reserve University, and the University of Akron. Support from the Chinese National Natural Science Foundation for promoting scientific collaborations is also acknowledged.

References and Notes

(1) Cheng, S. Z. D.; Yoon, Y.; Zhang, A.; Savitski, E. P.; Park, J.-Y.; Percec, V.; Chu, P. *Macromol. Rapid Commun.* **1995**, *16*, 533.
(2) Yoon, Y.; Zhang, A.; Ho, R.-M.; Cheng, S. Z. D.; Percec, V.; Chu, P. *Macromolecules* **1996**, *29*, 294.
(3) Yoon, Y.; Ho, R.-M.; Moon, B.; Kim, D.; McCreight, K. W.; Li, F.; Harris, F. W.; Cheng, S. Z. D.; Percec, V.; Chu, P. *Macromolecules* **1996**, *29*, 3421.
(4) Yoon, Y.; Ho, R.-M.; Savitski, E. P.; Li, F.; Cheng, S. Z. D.; Percec, V.; Chu, P. In *Liquid-Crystalline Polymer Systems Technological Advances*; ACS Symposium Series 632; American Chemical Society: Washington, DC, 1996; pp 358−371.
(5) Yoon, Y.; Ho, R.-M.; Li, F.; Moon, B.-S.; Park, J.-Y.; Harris, F. W.; Cheng, S. Z. D.; Percec, V.; Chu, P. *J. Therm. Anal.* **1996**, *47*, 957.
(6) Yoon, Y.; Ho, R.-M.; Li, F.; Leland, M.; Park, J.-Y.; Cheng, S. Z. D.; Percec, V.; Chu, P. *Prog. Polym. Sci.* **1997**, *22*, 765.
(7) Cheng, J.; Yoon, Y.; Ho, R.-M.; Leland, M.; Guo, M.; Cheng, S. Z. D.; Percec, V.; Chu, P. *Macromolecules* **1997**, *30*, 4688.
(8) Ho, R.-M.; Yoon, Y.; Leland, M.; Cheng, S. Z. D.; Yang, D.; Percec, V.; Chu, P. *Macromolecules* **1996**, *29*, 4528.
(9) Ho, R.-M.; Yoon, Y.; Lelend, M.; Cheng, S. Z. D.; Percec, V.; Chu, P. *Macromolecules* **1997**, *30*, 3349.
(10) Shadashiva, B. K.; Suresh, K. A. *Pramana* **1977**, *9*, 471.
(11) Destrade, C.; Malthete, J.; Tinh, N. H.; Gasparoux, H. *Phys. Lett.* **1980**, *78A*, 82.
(12) Destrade, C.; Tinh, N. H.; Gasparoux, H.; Malthete, J.; Levelut, A. M. *Mol. Cryst. Liq. Cryst.* **1981**, *71*, 111.
(13) Levelut, A. M.; Malthete, J. *Mol. Cryst. Liq. Cryst.* **1984**, *106*, 121.
(14) Malthete, J.; Levelut, A. M.; Tinh, N. H. *J. Phys. Lett.* **1985**, *46*, 875.
(15) Destrade, C.; Tinh, N. H.; Roubineau, A.; Levelut, A. M. *Mol. Cryst. Liq. Cryst.* **1988**, *159*, 163.
(16) Chandrasekhar, S.; Ranganath, G. S. *Rep. Prog. Phys.* **1990**, *53*, 57.
(17) Kreuder, W.; Ringsdorf, H.; Tschirner, P. *Makromol. Chem., Rapid Commun.* **1985**, *6*, 367.
(18) Ringsdorf, H.; Tschirner, P.; Herrmann-Schonheer, O.; Wendorff, T. H. *Makromol. Chem.* **1987**, *188*, 1431.
(19) Zheng, R.-Q.; Chen, E.-Q.; Cheng, S. Z. D.; Xie, F.; Yan, D.; He, T.; Percec, V.; Chu, P.; Ungar, G. *Macromolecules* **1999**, *32*, 3574.
(20) Percec, V.; Chu, P.; Ungar, G.; Cheng, S. Z. D.; Yoon, Y. *J. Mater. Chem.* **1994**, *4*, 719.
(21) Gray, G. W.; Goodby, J. W. G. *Smectic Liquid Crystals: Textures and Structures*; Leonard Hill: London, 1984.
(22) Pershan, P. S. *Structure of Liquid Crystal Phases*; World Scientific: Singapore, 1988.
(23) De Genes, P. G.; Prost, J. *The Physics of Liquid Crystals*; Oxford: New York, 1993.
(24) Chaikin, P. M.; Lubensky, T. C. *Principle of Condensed Matter Physics*; Cambridge: New York, 1995.
(25) Ungar, G. *Polymer* **1993**, *34*, 2050.
(26) Unger, G.; Feijoo, J. L.; Percec, V.; Yourd, R. *Macromolecules* **1991**, *24*, 953.
(27) Yandrasits, A.; Cheng, S. Z. D.; Zhang, A.; Cheng, J.; Wunderlich, B.; Percec, V. *Macromolecules* **1992**, *25*, 2112.
(28) Pardey, R.; Harris, F. W.; Cheng, S. Z. D.; Adduci, J.; Facinelli, J. V.; Lenz, R. W. *Macromolecules* **1992**, *25*, 5060.
(29) Pardey, R.; Shen, D.; Gabori, P. A.; Harris, F. W.; Cheng, S. Z. D.; Adduci, J.; Facinelli, J. V.; Lenz, R. W. *Macromolecules* **1993**, *26*, 3687.

MA9910235